Invisible Random Media and Diffraction Gratings that don't Diffract

C. G. King, S. A. R. Horsley, and T. G. Philbin

Department of Physics and Astronomy, University of Exeter, Stocker Road, Exeter, EX4 4QL

Graded index media whose electric susceptibility satisfies the spatial Kramers-Kronig relations are shown to be one-way reflectionless to electromagnetic radiation, for all angles of incidence. We demonstrate how a family of these media, in addition to being reflectionless, also have negligible transmission, hence maximising the absorption of the wave's energy. On a different note, the transmission of a wave through a randomly chosen 'pile of plates' typically decreases exponentially with the number of plates, a phenomenon closely related to Anderson localisation. In apparent contradiction we construct disordered planar permittivity profiles which are real-valued, two-way reflectionless and perfectly transmitting for a single angle of incidence and a narrow frequency range. This behaviour is confirmed by numerical simulations. Finally, by mapping out the behaviour of phase fronts, we have designed two dimensional graded-index media which don't scatter at all. In particular, we have designed a medium which behaves as a 'beam-shifter' at a single frequency; acting to laterally shift a plane wave, or sufficiently wide beam, without reflection. Additionally, we have designed a periodic grating for which diffraction is completely suppressed at a single frequency at normal incidence to the periodicity.

INTRODUCTION

Wave propagation through inhomogeneous media cannot be solved analytically in most cases, even in one dimension. There are a small number of cases which can be solved exactly, such as the non-reflecting Pöschl-Teller profiles [1, 2]. However, the space of possible media is too large to be able to calculate reflection and transmission coefficients numerically in all cases. Instead, mathematical techniques can be used to make progress, particularly with a view to designing non-scattering media.

Consider the situation of a monochromatic wave of frequency ω incident on a linear isotropic material whose permittivity varies only along one direction, as shown in figure 1. The electric field φ corresponding to
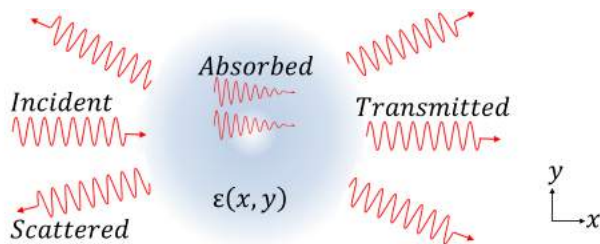
FIG. 1: A wave of wavenumber $k_0 = \omega/c$ is incident from the negative x axis upon a material whose permittivity may be described by $\epsilon(x)$ and is spatially homogeneous along the y direction. In general it is expected that the incident wave will split into three parts: a reflected wave, a transmitted wave and a part absorbed into the medium.

a TE polarised plane wave propagating in the (x, y)-plane through a material uniform in the y direction with permittivity $\epsilon(x)$ and unit permeability satisfies the

Helmholtz equation

$$\left[\frac{d^2}{dx^2} + k_0^2 \epsilon(x) - k_y^2 \right] \varphi(x) = 0. \tag{1}$$

Here $k_0 = \frac{\omega}{c}$ and k_y determines the angle of incidence of the wave. In what follows it is assumed without loss of generality that $k_y = 0$ (setting $k_y = 0$ corresponds to normal incidence; a non-zero k_y merely shifts the background value of the effective 1d permittivity). Considering the situation of a medium sitting in free space, it is natural to split the permittivity up into its background value ϵ_{vac} (which from now on will be taken as unity) and the electric susceptibility χ containing the inhomogeneous part $\epsilon(x) = \epsilon_{\text{vac}} + \chi(x)$.

SPATIAL KRAMERS-KRONIG RELATIONS AND THE REFLECTIONLESSNESS OF LEFT INCIDENT WAVES:

This section is based on work in [4].

Consider Helmholtz's equation (1) being analytically continued to a complex position $z = x_1 + ix_2$, $\epsilon(z) = 1 + \chi(z)$. There are a special class of profiles that are analytic on one half of the complex position plane [3, 4]. These satisfy the spatial Kramers-Kronig relations [5]

$$\begin{aligned} \text{Re}(\chi(x)) &= \frac{1}{\pi} \mathbb{P} \int_{-\infty}^{\infty} \frac{\text{Im}(\chi(x'))}{x' - x} dx' \\ \text{Im}(\chi(x)) &= -\frac{1}{\pi} \mathbb{P} \int_{-\infty}^{\infty} \frac{\text{Re}(\chi(x'))}{x' - x} dx'. \end{aligned} \tag{2}$$

Consider a wave propagating left-to-right through the medium. The analytic continuation of the transmitted wave along the large semi-circle of the complex position plane is shown in figure 2. The asymptotic behaviour of the solution in vacuum at an angle θ can be written as a combination of left and right propagating waves
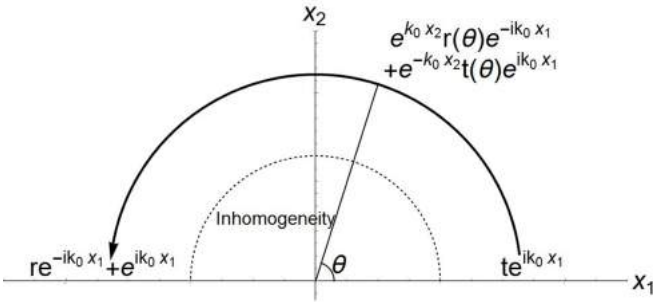
FIG. 2: On the far right of the profile, the asymptotic form of the wave can be analytically continued into the upper half position plane. The right-going wave is exponentially diminished while the left-going wave is exponentially amplified.

$t(\theta)\mathrm{e}^{\mathrm{i}k_0 z} + r(\theta)\mathrm{e}^{-\mathrm{i}k_0 z}$. A non-zero reflection coefficient $r(\theta)$ leads to an exponentially growing solution as the semi-circle radius is increased. However, as the solution must be analytic in this upper half plane, and the susceptibility decays to zero, there cannot be a discontinuity in the asymptotic behaviour of the solution, which would be required by a non-zero reflection coefficient, thus explaining why the reflection coefficient must vanish.

Without the requirement of analyticity in the upper half plane, this argument breaks down due to the presence of branch cuts crossing the semicircular path of figure 2, across which the asymptotic expansion of the solution in terms of plane waves is discontinuous [3]. This leads to a Stokes phenomenon- the presence of differing asymptotic expansions in different regions of the complex plane [6]. Having this analyticity condition removes the Stokes phenomenon, and hence any reflected wave.

By replacing the left and right propagating plane waves with the more accurate WKB waves [6]

$$\frac{1}{\epsilon(z)^{1/4}}\mathrm{e}^{\pm \mathrm{i}k_0 \int_a^z \sqrt{\epsilon(\hat{z})}d\hat{z}} \qquad (3)$$

and keeping track of the zero phase reference point, a, as it moves along the semi-circle with the solution, the transmission coefficient can be calculated, in the limit as semi-circle radius tends to infinity, as

$$t = \mathrm{e}^{\mathrm{i}k_0 \int_{-\infty}^{\infty} \sqrt{\epsilon(x)}dx}. \qquad (4)$$

PERFECTLY ABSORBING MEDIA

This section is based on the work in [7].

Transformation optics can also be used to design perfect absorbers. For example, perfectly matched layers (PMLs) [8] are commonly used in numerical simulations to absorb waves without reflection. However, they generally consist of an anisotropic permittivity and permeability, making them difficult to realise practically. In this work, non-reflecting, non-transmitting, isotropic graded index media are designed, based on the work of the previous section. An experimental realisation of near perfect absorbers based on these media has been carried out in [9].

Having obtained the transmission coefficient for spatial Kramers-Kronig media, the conditions for obtaining zero transmission (and hence perfect absorption) can be obtained. Consider a subset of the class of spatial Kramers-Kronig media: permittivity profiles containing a finite number of poles in the lower half position plane:

$$\epsilon(z) = 1 + \sum_{k=1}^{N_1} \frac{a_{1,k}}{z - z_{1,k}} + \sum_{k=1}^{N_2} \frac{a_{2,k}}{(z - z_{1,k})^2} + ... \qquad (5)$$

Integrating around a large semi-circle C in the upper half plane contributes half a residue from each of the simple poles leading to a transmission coefficient [4]

$$|t| = \mathrm{e}^{\frac{1}{2}\pi k_0 \mathrm{Re} \sum_{k=1}^{N_1} a_{1,k}}. \qquad (6)$$

It is therefore clear how to make graded index permittivity profiles having any desired transmission coefficient between 0 and 1 by tuning the residues of simple poles in ϵ. However, it is not clear how to make the transmission coefficient negligible without taking the limit of one of the simple pole residues going to $-\infty$ (and hence the imaginary part of the permittivity to ∞). In the rest of this work, we explore how to make the transmission coefficient negligible whilst keeping the permittivity bounded.

High absorption has been achieved experimentally by a metamaterial having a profile of the form (5) where the number of poles n is finite [9]. However, for these spatial Kramers-Kronig media, to make the transmission coefficient completely vanish and have all of the incident wave absorbed, it follows from (6) that we require a profile where the sum of the residues is infinite

$$\sum_k \mathrm{Re}(a_{1,k}) = -\infty. \qquad (7)$$

The transmission coefficient can be classified in terms of the decay of the susceptibility in the following way:

$$\begin{aligned} |t| = 1 \qquad &\text{if } \chi(x) < \mathrm{O}(1/x) \text{ as } x \to \infty \\ 0 < |t| < 1 \qquad &\text{if } \chi(x) = \mathrm{O}(1/x) \text{ as } x \to \infty \\ |t| = 0 \qquad &\text{if } \chi(x) > \mathrm{O}(1/x) \text{ as } x \to \infty. \end{aligned} \qquad (8)$$

As an example of this, consider taking $a_{1,k} = -\frac{\alpha}{k}$ and $z_{1,k} = -\beta k \mathrm{i}$ where α and β are positive constants. This corresponds to the profile

$$\epsilon(x) = 1 - \frac{\alpha}{x}\left(\gamma + \psi\left(1 - \frac{\mathrm{i}x}{\beta}\right)\right), \qquad (9)$$

where $\psi(x)$ is the digamma function (the logarithmic derivative of the Γ function) and γ is Euler's constant.

Having constructed this function from an infinite number of simple poles, note that asymptotically

$$\epsilon(x) = 1 - \frac{\alpha \ln x}{x} + O\left(\frac{1}{x}\right) \qquad \text{as } x \to \pm\infty, \qquad (10)$$

so here it is the weaker $\ln(x)/x$ decay which leads to a profile with zero transmission. Since all terms beyond the second term do not affect the transmission (see (5) and (6)), for simplicity consider the profile obtained by neglecting the $O(1/x)$ part of (10) and displacing the remaining singularity to the lower half plane (which merely causes an $O(1/x)$ alteration in the profile):

$$\epsilon(x) = 1 - \frac{\alpha \ln(\frac{x}{a} + \delta i)}{\frac{x}{a} + \delta i}, \qquad (11)$$

where δ and a are positive constants. This preserves the required property of being analytic in the upper half complex position plane, therefore satisfying the spatial Kramers-Kronig relations. Wave propagation through such a material is simulated in figure 3 where the material has been spatially truncated on either side at $\pm 8\lambda$.

PERFECTLY TRANSMITTING DISORDERED MEDIA

This section is based on the work in [11] (see also [12] for a similar treatment).

A wave propagating through N randomly chosen lossless slabs of material tends to be exponentially extinguished as N increases [13, 14]. The transmission through such a random combination of slabs is given by the geometric mean of the transmissivity, $|t_{\text{eff}}|^2 = \exp(2\langle \log(|t|)\rangle)$ corresponding to averaging over all possible realisations. For N slabs this is [13]

$$|t_{\text{eff}}|^2 = \exp\left(-2\sum_{i=1}^{N}\left\langle \log\left(\frac{1}{|t_i|}\right)\right\rangle\right), \qquad (12)$$

where t_i is the transmission coefficient for the ith slab). The average transmissivity (12) clearly decreases exponentially with increasing N (see [15] for bounds), leading to the phenomenon where a layered transparent disordered medium tends to act as a good mirror. Families of layered media with permittivities that are similarly random in the direction of propagation are constructed and yet the expected high reflection and low transmission is avoided. This is connected to the phenomenon of Anderson (strong) localisation, which predicts that the eigenstates of a given disordered lattice will tend not to extend over the entire lattice, but will be localised around each of the sites [16, 17].

Importantly this implies that such profiles consisting of poles of order two or higher (so $N_1 = 0$ in (5)) exhibit zero reflection and perfect transmission *regardless* of their
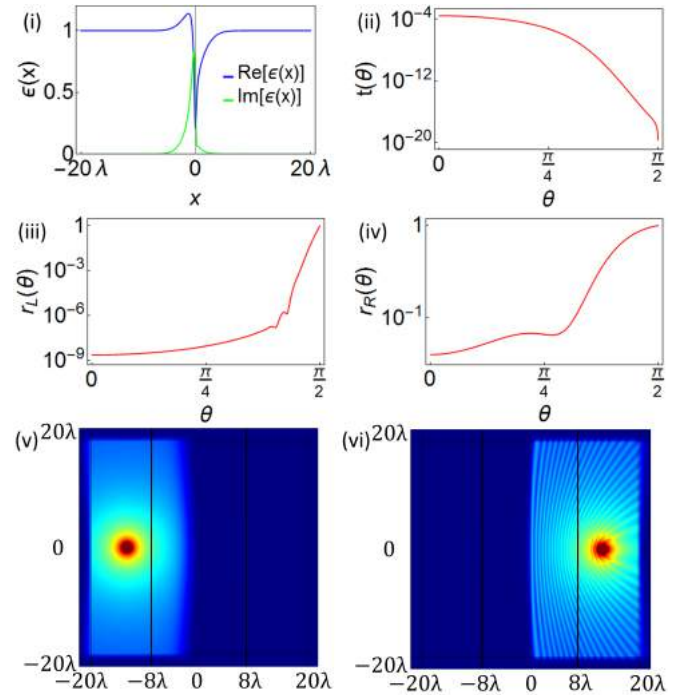
FIG. 3: (i) The real and imaginary parts of the permittivity profile $\epsilon(x) = 1 - \frac{\ln(k_0 x + 2i)}{k_0 x + 2i}$, truncated at $x = \pm 50/k_0$. (ii) The transmission coefficient on a logarithmic scale of a plane wave propagating in either direction through the medium as a function of incidence angle. (iii) and (iv) The reflection coefficient for left and right incidence, respectively, as a function of incidence angle. (v) and (vi) Wave propagation simulated in Comsol Multiphysics [10] by placing an out-of-plane line source to the (ii) left and (iii) right of the medium and the time-average of the absolute value of the electric field is plotted. Reflection and transmission is suppressed for a left incident wave whereas just the transmission is suppressed for a right incident wave.

number N_j, weight $a_{j,k}$ or position $z_{j,k}$ in the lower half plane ($\text{Im}(z_{j,k}) < 0$). See [3] for a simulation of the wave propagation through the permittivity corresponding to a single double pole on the negative imaginary axis. More generally, perfect transmission can be achieved when the complex function $\chi(x)$ both satisfies (2) and integrates to zero over the real line,

$$\int_{-\infty}^{\infty} \chi(x)dx = 0 \qquad (13)$$

a requirement found in [4, 18] and referred to by Longhi as the 'cancellation condition' (see [19]). For profiles given by (5), the cancellation condition is equivalent to only having poles of order two, or higher, and is guaranteed to give perfect transmission. To obtain real-valued perfectly transmitting media, the technique of Berry and Howls [20] is applied, where the following ansatz for φ is

substituted into equation (1)

$$\varphi(x) = \frac{1}{p(x)^{1/4}} \exp\left(\pm i\kappa \int^{x} dx' \sqrt{p(x')}\right) \qquad (14)$$

which is based on the form of the WKB solutions given in e.g. [6]. The two possible signs in the exponent correspond to right and left travelling waves propagating without reflection, with unit transmission when $p(x)$ is real and tending to 1 at $x \to \pm\infty$. Upon substitution of (14) into the Helmholtz equation (1), one can solve for the requisite permittivity profile, which is found to be

$$\epsilon(x, \kappa) = p(x) - \frac{p(x)^{1/4}}{\kappa^2} \frac{d^2}{dx^2} \left(\frac{1}{p(x)^{1/4}}\right). \qquad (15)$$

Equation (15) gives a recipe for the construction of real-valued permittivity profiles that are reflectionless at normal incidence, for fixed κ. By choosing $p(x)$ as a randomly varying function (with a rapidly decaying two-point correlation function and a Hurst exponent close to 0.5), we obtain a similarly randomly varying permittivity profile that exhibits perfect transmission at the wavenumber $k_0 = \kappa$. An example of this is shown in figure 4, where $p(x)$ is defined as a finite (but long) Fourier sine series with compact support

$$p(x) = 1 + \begin{cases} \sum_{n=1}^{N} a_n \sin\left(\frac{n\pi x}{L}\right), & 0 < x < L \\ 0, & \text{otherwise} \end{cases} \qquad (16)$$

and the coefficients are chosen randomly in such a way that $\sum_{i=1}^{\lfloor \frac{n-1}{2} \rfloor} (n - 2i) a_{n-2i}$ is taken from a symmetric real uniform distribution for $n = 1, 2, ..., N - 2$ and is vanishing for $n = N - 1, N$. This ensures the smoothness of p, and hence the continuity of ϵ. An example is shown in figure 4.

WAVE PROPAGATION IN TWO DIMENSIONS

Solving the problem of wave propagation in two dimensions is, unsurprisingly, a more difficult problem than the one-dimensional analogue. With the extra complications, however, comes a greater range of practical possibilities, such as beam bending, shifting or focussing, as well as cloaking. It is common to use ray tracing (see for example [21]) to manipulate the path of propagation of the light. For example, radial index profiles, such as the Luneburg lens [22], can be used to focus light from a plane wave to a single point. However, such an approach relies on the validity of the geometrical optics approximation, which will break down near the focus of the rays. By considering the exact wave problem, such difficulties are bypassed enabling a greater control of the sort of frequencies our media can function at. Transformation optics using conformal mapping [23, 24] has been at the forefront of recent developments; in particular motivating
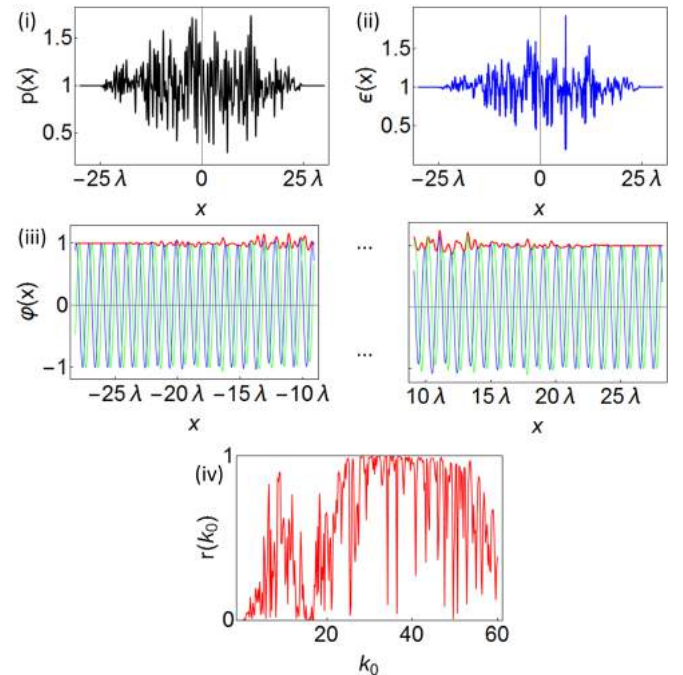
FIG. 4: (i) A particular choice of $p(x)$ given by (16) with $N = 250$. (ii) The corresponding permittivity when $\kappa = 5\pi$. (iii) Time-averaged (red, upper) amplitude of a left incident wave of wavenumber κ, propagating through a medium with permittivity $\epsilon(x, \kappa)$. Real and imaginary parts of the wave are shown in blue and green, respectively. The lack of oscillations in (iii) indicates that the profile is reflectionless for this wave. The wave is also transmitted without a change in amplitude or a shift in phase. (iv) The reflection as a function of wavenumber k_0. The reflection coefficient is very sensitive to the frequency of the incident wave and high reflection is possible except in a region about $k_0 = \kappa$ where the reflection is negligible.

the possibility of cloaking as has extensively been tested experimentally (see for example [25, 26]).

In two dimensions, the out-of-plane component of the electric field corresponding to a monochromatic Transverse Electric (TE) polarised wave of frequency ω incident upon a medium with real-valued permittivity ϵ satisfies the two-dimensional Helmholtz equation

$$\left[\nabla^2 + k_0^2 \epsilon\right] \varphi = 0. \qquad (17)$$

Instead of attempting to solve directly, it is convenient to rewrite the solution in terms of its real-valued amplitude A and phase S as $\phi = A(x, y)e^{ik_0 S(x,y)}$. Upon substitution back into (17) and separation into real and imaginary parts, the following equations result:

$$\begin{aligned} \epsilon &= (\nabla S)^2 - \frac{\nabla^2 A}{k_0^2 A} \\ 0 &= \nabla \cdot (A^2 \nabla S). \end{aligned} \qquad (18)$$

Special cases in which geometrical optics gives the exact solution are explored in [27] i.e. when the 'quan-

tum potential' term $\frac{\nabla^2 A}{A}$ vanishes. Instead, here we start with solving this second equation, and use the first to obtain the corresponding permittivity. The divergence free quantity $A^2 \nabla S$ is exactly proportional to the time-averaged Poynting vector (more precisely $\mathbf{S} = \frac{1}{2\mu_0} A^2 \nabla S$), and this equation is simply an energy conservation equation expressing the assumption that no current sources are present in the medium.

THE BEAM-SHIFTER:

Beam-shifters have largely been designed using the coordinate transformations of transformation optics contained in [23] using anisotropic media with graded permittivity and permeability tensors (see for example [28–30]). Instead an isotropic permittivity profile which laterally shifts a beam at a single frequency with negligible reflection is proposed.

There are a small number of special cases where the energy conservation equation can be solved exactly to give a permittivity profile with an interesting properties. Here, a wide beam is laterally shifted without reflection and will henceforth be referred to as the beam-shifter. The energy conservation condition in one dimension

$$\frac{d}{dx}\left(A^2 \frac{dS}{dx}\right) = 0. \tag{19}$$

can immediately be integrated up to give

$$A = \frac{A_0}{\sqrt{\frac{dS}{dx}}}. \tag{20}$$

It is then common to take the geometrical optics limit $k_0 \gg |\nabla \epsilon|/\epsilon^{3/2}$, where the remaining equation is simply the eikonal equation $\epsilon = \left(\frac{dS}{dx}\right)^2$ to get the WKB approximations [6]. In this case, however, progress can be made in two dimensions without resorting to such approximations. Motivated by being able to solve the conservation of energy equation in one dimension, it is natural to solve the analogous two dimensional equation for a special case by imposing that the second equation of (18) holds for each of the individual coordinates. i.e.

$$\frac{\partial}{\partial x}\left(A^2 \frac{\partial S}{\partial x}\right) = 0$$
$$\frac{\partial}{\partial y}\left(A^2 \frac{\partial S}{\partial y}\right) = 0. \tag{21}$$

which can be solved separately to give two expressions for the amplitude:

$$A = \frac{A_y(y)}{\sqrt{\frac{\partial S}{\partial x}}} = \frac{A_x(x)}{\sqrt{\frac{\partial S}{\partial y}}}. \tag{22}$$

This can then be subsequently solved for the phase:

$$S = f(X(x) + Y(y)). \tag{23}$$

where $X' = 1/A_x^2$ and $Y' = 1/A_y^2$. The particularly neat thing about this idea of separating the equations for the different Cartesian coordinates is that the differential equation for the rays takes a separable form

$$\frac{dy}{dx} = \frac{Y'(y)}{X'(x)}. \tag{24}$$

and, in particular, by taking $Y(y) = y$, say, the slope of the rays depends only on the x coordinate and thus the rays are translationally invariant in the y direction, as one would expect for a beam-shifter. Meanwhile (18) gives the expression for the permittivity

$$\begin{aligned}
\epsilon = &(f')^2 \left((X')^2 + (Y')^2\right) \\
&+ \frac{1}{2k_0^2}\left[\frac{X'''}{X'} + \frac{Y'''}{Y'} - \frac{3}{2}\left(\frac{(X'')^2}{(X')^2} + \frac{(Y'')^2}{(Y')^2}\right)\right] \\
&+ \frac{1}{2k_0^2}\left[\left((X')^2 + (Y')^2\right)\left(\frac{f'''}{f'} - \frac{3(f'')^2}{2(f')^2}\right)\right].
\end{aligned} \tag{25}$$

where only the first line would be retained in the geometrical optics limit. As for the periodic grating, our medium should sit in free space with a right propagating plane wave incident on the medium emerging totally as a right propagating plane wave without being scattered. To ensure that the rays are horizontal either side of the medium ($X' \to +\infty$ as $x \to \pm\infty$), we choose, as a simple example,

$$\begin{aligned}
X(x) &= \frac{\sinh(\alpha x)}{\alpha} \\
Y(y) &= y.
\end{aligned} \tag{26}$$

leading to rays $y = \frac{2}{\alpha}\arctan\left(\tanh\left(\frac{\alpha x}{2}\right)\right) + $constant which bend and straighten with a lateral shift of π/α, as shown in figure 5(i). To further ensure a right propagating plane wave either side of the medium, it is required that $S \sim x$ as $x \to \pm\infty$ so it is natural to choose f to be the inverse of X:

$$f(z) = X^{-1}(z) = \frac{\text{arsinh}(\alpha z)}{\alpha}. \tag{27}$$

and we again choose a wavenumber of $k_0 = 10$. With these choices the permittivity profile obtained is shown in figure 5(ii) and is given by

$$\epsilon(x,y) = \frac{1 + \cosh^2(\alpha x)}{1 + (\alpha y + \sinh(\alpha x))^2} + \text{O}\left(\frac{1}{k_0^2}\right). \tag{28}$$

where the correction terms to the geometrical optics limit have been included in the plot but have been left out of (28) for brevity. The resulting shift in the beam can then be seen in a plot of the field norm, as shown in figure 5(iii).

of equations should be solved simultaneously:

$$\frac{\partial x}{\partial \lambda} = \frac{\partial S}{\partial x}$$
$$\frac{\partial y}{\partial \lambda} = \frac{\partial S}{\partial y} \tag{30}$$
$$\frac{\partial A}{\partial \lambda} = -\frac{A}{2}\nabla^2 S.$$

Together with suitable boundary conditions, the resulting parametric solution will map out a surface in (x, y, A) space. The first two equations decouple from the third and can be numerically solved to map out the rays (or characteristics) in the (x, y) plane with the parameter λ parameterising each ray (as can be seen by taking their ratio $\frac{dy}{dx} = \frac{\partial_y S}{\partial_x S}$). The different rays are parameterised by a different parameter, μ say, depending on the specific form of the boundary condition. The situation is described visually in figure 6.
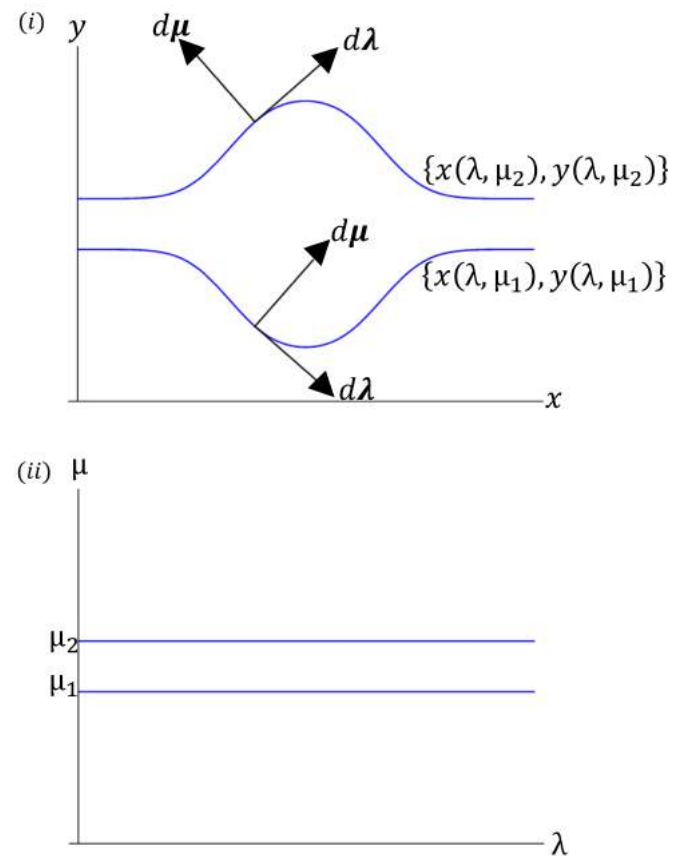
FIG. 6: Plots of two of the rays in (i) (x, y) space, and (ii) (λ, μ) space. (λ, μ) defines a coordinate system in which the rays are straight lines of constant μ. λ parameterises each ray whilst μ parameterises the different rays. In (λ, μ) space, the equation for amplitude becomes a simple ODE.

As a boundary condition, a uniform amplitude is imposed along a vertical line $x =$constant on the left (incident) side of the medium. Together with a suitable choice

FIG. 5: (i) The rays associated with the choices given in (26) with $\alpha = 1$. (ii) The corresponding permittivity profile with $f = X^{-1}$ and $k_0 = 10$ in $-5 < x < 5$ and free space either side. (iii) The field norm corresponding to a right propagating incident Gaussian beam of width 4, simulated using Comsol Multiphysics [10]. The wave is transmitted with negligible reflection and with a beam shift of π.

NON-DIFFRACTING PERIODIC GRATINGS:

In order to guide a wave through a medium in some desired fashion (i.e. along a particular set of rays) it is sufficient to specify the phase $S(x, y)$ of the wave inside the medium. The conservation of energy condition then tells us the corresponding amplitude distribution required to achieve such a propagation though a lossless medium. By explicitly writing out the energy conservation equation as

$$\frac{\partial S}{\partial x}\frac{\partial A}{\partial x} + \frac{\partial S}{\partial y}\frac{\partial A}{\partial y} = -\frac{A}{2}\nabla^2 S, \tag{29}$$

it becomes of the form for which the method of characteristics may be applied (see, for example, [31] for a discussion of this method). Therefore the following set

of phase S, this will correspond to a right propagating plane wave without reflection.

Consider a plane wave propagating in the positive x direction impinging on a medium periodic in the y direction, with periodicity $a = 2\pi/k_g$ and sitting in free space: $\epsilon \to 1$ as $x \to \pm\infty$. Such a periodic medium will typically produce a diffraction pattern, the field being the sum of waves propagating in different directions. Relative to an angle of incidence θ_i with the positive x axis, the possible angles for waves to scatter away from the medium are

$$\sin\theta_n = \sin\theta_i + \frac{nk_g}{k_0}. \tag{31}$$

and the corresponding reflection and transmission coefficients can be written as

$$
\begin{aligned}
R_n &= \frac{\sqrt{k_0^2 - (k_y + nk_g)^2}}{k_x} |\varphi_{r,n}|^2 \\
T_n &= \frac{\sqrt{k_0^2 - (k_y + nk_g)^2}}{k_x} |\varphi_{t,n}|^2.
\end{aligned}
\tag{32}
$$

where $\mathbf{k}_0 = k_x\hat{\mathbf{x}} + k_y\hat{\mathbf{y}}$. The situation is described visually in figure 7.
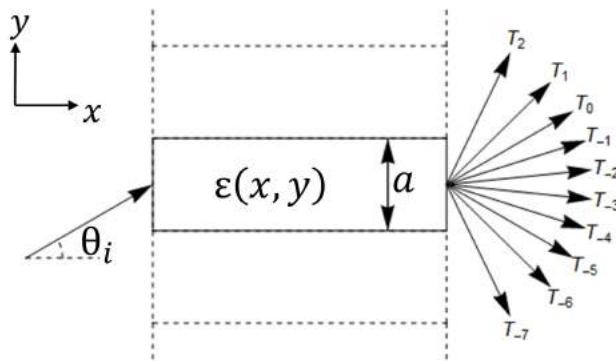
FIG. 7: A wave incident from the left upon a permittivity profile $\epsilon(x,y)$ periodic in the y direction with period a. The resulting diffraction pattern consists of a superposition of waves reflected and transmitted at various angles with intensities given by equation (32) (the reflected waves aren't shown in this diagram to avoid cluttering).

Consider designing a profile for which diffraction is suppressed for a particular wavenumber at normal incidence to the periodicity (i.e. $\theta_i = 0$). Then, for a right propagating plane wave with perfect transmission without reflection, the phase should asymptotically satisfy $S \sim x$ as $x \to \pm\infty$, and any distortion in the rays should be contained within the medium. To this end we make the following choice of phase. In the region $-\frac{a}{2} < y < \frac{a}{2}$, let

$$
\begin{aligned}
S = &\, x + b\,\mathrm{erf}\left(\frac{x}{c}\right) \\
&+ \alpha x e^{-\left(\frac{x}{d}\right)^2}\left[1 + \mathrm{erf}\left(\frac{\frac{a}{4}+y}{h}\right)\mathrm{erf}\left(\frac{\frac{a}{4}-y}{h}\right)\right],
\end{aligned}
\tag{33}
$$

where $\mathrm{erf}(z) = \frac{2}{\sqrt{\pi}}\int_0^z e^{-\tilde{z}^2}d\tilde{z}$ is the error function, which switches smoothly from -1 to $+1$ with increasing argument. This is then repeated periodically up and down the y axis. The characteristic method can then be used to numerically find the rays, as shown in figure 8(i). Notice
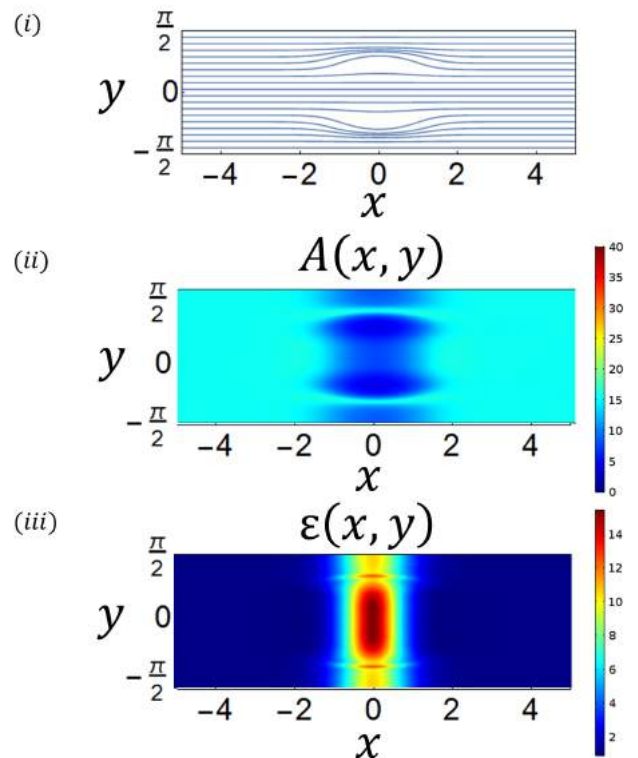
FIG. 8: (i) The rays corresponding to the phase distribution given in (33) in a 'unit cell' where $a = \pi, b = 2, c = 1, d = 1, h = 1/4$ and $\alpha = 1/3$. (ii) The corresponding amplitude resulting from solving the characteristic equations (30). (iii) The corresponding permittivity profile as determined from the first equation of (18) corresponding to $k_0 = 10$.

that the dependence of the medium transverse to the direction of propagation acts to distort the rays. However, upon propagation through the medium, the rays respace evenly again. In particular, this means that a plane wave incident upon the medium will emerge as a plane wave. This has been done by solving the final equation of (30) subject to the boundary condition $A \to 1$ as $x \to -\infty$. The amplitude is plotted in figure 8(ii). The uniformity of the amplitude either side of the medium implies that a monochromatic plane wave propagates through the medium without scattering (whether in the form of reflection or diffraction). Up to this point the choice of frequency hasn't needed to be made. However, to obtain the permittivity profile using (18), a choice now must be made. We have chosen a free space wavenumber of $k_0 = 10$. Bearing in mind the periodicity of the medium, this value ensures that diffraction should be possible (in-

deed the first four diffracted modes should be visible), so that the absence of diffraction is a surprising result, but not so high that the absence of reflection can be put down to being in the geometrical optics limit. The corresponding permittivity profile is plotted in figure 8(iii). As expected, the permittivity approaches that of free space as $x \to \pm\infty$ with a range of unity up to around 15 in the medium.

The design process of such a non-scattering medium is such that it is only expected to function for an incident plane wave of frequency $\omega = ck_0 = 10c$. For other frequencies there is no reason not to expect a large amount of scattering in the form of both reflection and diffraction. We have investigated the effect of sending in different frequencies of radiation through the permittivity profile. Some plots of the electric field norm are shown in figure 9. Except at the wavenumber for which the medium is de-
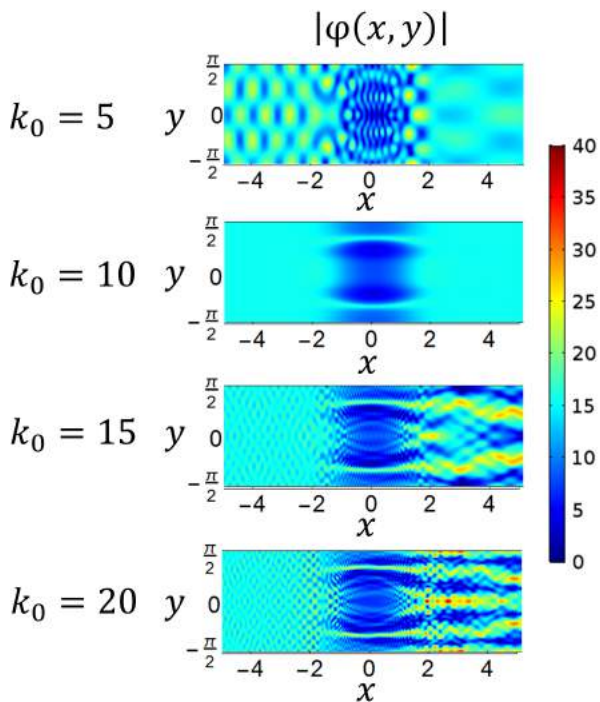
FIG. 9: The electric field norm corresponding to a plane wave propagating in the positive x direction through the permittivity profile of figure 8(iii) at four different wavenumbers, simulated using Comsol Multiphysics [10]. As expected the field amplitude is uniform at the wavenumber $k_0 = 10$ designed to give no scattering whereas diffraction is visible at other wavenumbers.

signed to be non-scattering, we see intricate diffraction patterns on both the incident and transmitted sides of the medium, with the fineness of the pattern being on the order of the wavelength. Upon calculation of the reflected and transmitted intensities going into each mode using (32), plots of the intensities as a function of wavenum-

ber can be obtained and are shown for this example in figure 10. For ($k_0 < 2$), the wavelength is longer than
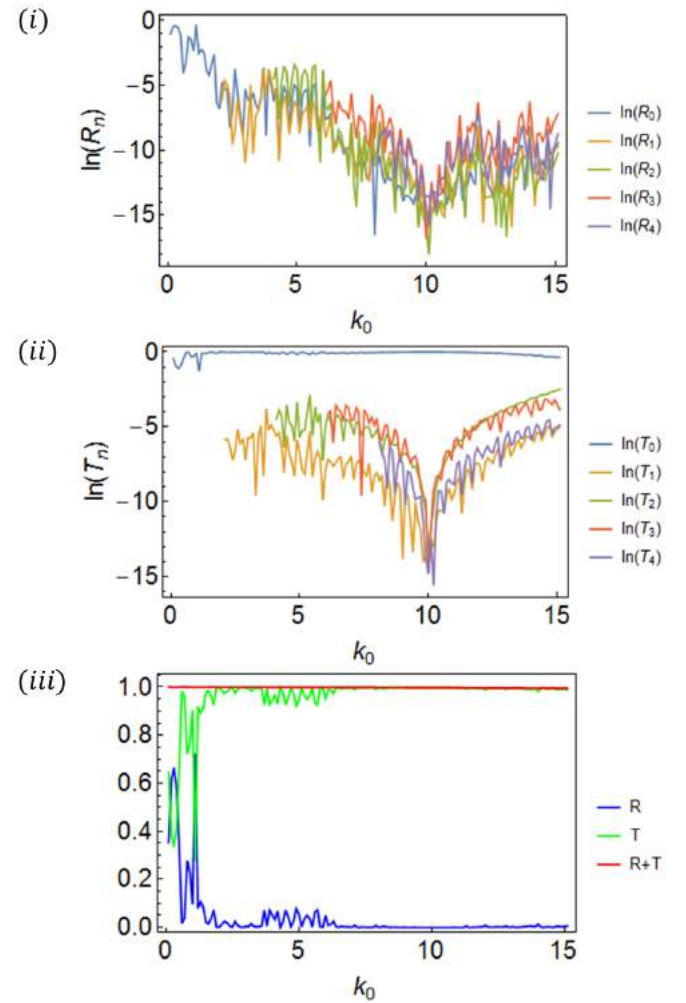
FIG. 10: The natural logarithm of the (i) reflected and (ii) transmitted intensities of the first five non-negative diffracted modes that a right propagating plane wave impinging on the permittivity profile of figure 8(iii) at normal incidence scatters into as a function of wavenumber. (iii) The total reflected (R) and transmitted (T) intensities and their sum. Almost all of the wave ends up being transmitted through in a broadband around $k_0 = 10$.

the periodicity, diffraction is not possible and so only the zero order modes corresponding to lateral transmission and reflection are possible. As k_0 is increased beyond 2, diffraction is expected and energy is carried via the lower order modes via both reflection and transmission. It is clear from these plots that, in general, these intensities fluctuate very rapidly as the wavenumber is altered through different sharp resonances. However, there is a noticeable broader-band dip in all but the zero order transmitted mode (the unscattered mode) around the wavenumber $k_0 = 10$ at which the structure is designed to be reflectionless and perfectly transmitting.

SUMMARY AND CONCLUSIONS:

We have designed reflectionless permittivity profiles satisfying the spatial Kramers-Kronig relations, in particular showing how they can be made into perfect absorbers. The findings were numerically verified for a finite slab of material using Comsol Multiphysics [10]. We have also explored real-valued permittivity profiles that appear to have been generated by a random walk-like process yet exhibit unit transmission and zero reflection in a narrow band of frequency and a particular incidence angle, thus avoiding Anderson localisation. Finally, by considering ways of solving the local conservation of energy equation in terms of amplitude and phase for lossless media in two dimensions, we have derived a recipe for designing 'beam-shifters'; graded-index permittivity profiles which laterally shift a Gaussian beam of at least a few wavelengths, without reflection, and a recipe for designing periodic graded-index permittivity profiles which suppress diffraction.

ACKNOWLEDGEMENTS:

————————

[1] P. S. Epstein, *Proc. Nat. Acad. Sci.* **10**, 627 (1930).
[2] J. Lekner, *Am. J. Phys.* **75**, 1151 (2007).
[3] S. A. R. Horsley, M. Artoni and G. C. La Rocca, *Nature Phot.* **9** 436 (2015).
[4] S. A. R. Horsley, C. G. King and T. G. Philbin, *J. Opt.* **18** 4 (2016).
[5] L. D. Landau and E. M. Lifshitz, *Statistical Physics*, Pergamon, (1969).
[6] J. Heading, *An Introduction to Phase-Integral Methods*, Dover, (2013).
[7] C. G. King, S. A. R. Horsley and T. G. Philbin, *J. Opt.* **19**, 085603, (2017).
[8] J. Berenger, *J. Comp. Phys.* **114**, 185, (1994).
[9] W. Jiang et. al., *Laser and Phot. Rev.* **11**, 1, (2017).
[10] COMSOL Multiphysics v. 5.1. www.comsol.com. COMSOL AB, Stockholm, Sweden.
[11] C. G. King, S. A. R. Horsley and T. G. Philbin, *Phys. Rev. Lett.* **118** 163201 (2017).
[12] K. G. Makris et.al., *Light: Sci. & Apps.* **6**, e17035, (2017).
[13] M. V. Berry and S. Klein, *Eur. J. Phys.* **18**, 3, 222–228, (1997).
[14] V. Baluni and J. Willemsen, *Phys. Rev. A* **31**, 3358, (1985).
[15] Y. Lu, C. Miniature and B.-G. Englert, *Eur. J. Phys.* **31**, 47, (2009).
[16] P. W. Anderson, *Phys. Rev.* **109** 1492 (1958).
[17] P. W. Anderson, *Nobel Media AB 2014*, (1977).
[18] S. Longhi, *Europhysics Letters*, **112** 6 (2015).
[19] H. Kober, *Bull. Amer. Math. Soc.* **48** 6 (1942).
[20] M. V. Berry and C. J. Howls, *J. Phys. A* **23**, 6, (1990).
[21] U. Leonhardt and T. G. Philbin, 2010, *Geometry and Light: The Science of Invisibility* (Dover Publications).
[22] R. K. Luneburg, 1944 *Mathematical Theory of Optics* (Providence, RI: Brown Univ. Press.).
[23] J. B. Pendry, D. Schurig and D. R. Smith, *Science* **312**, 5514, (2006).
[24] U. Leonhardt, *Science* **312**, 5781, (2006).
[25] N. Kundtz, D. Gaultney and D. R. Smith *New. J. Phys.* **12**, 043039, (2010).
[26] D. Schurig, J. J. Mock, B. J. Justice, S. A. Cummer, J. B. Pendry, A. F. Starr and D. R. Smith, *Science* **314**, 5801, (2006).
[27] T. G. Philbin, *J. Mod. Opt.*, **61**, 552, (2014).
[28] M. Y. Wang et.al., *Prog. Elec. Res.* **83**, 147, (2008).
[29] M. Salmasi, M. Okoniewski, M. E. Potter, *2016 IEEE Int. Symp. Antennas and Propagation* 725, (2016).
[30] A. M. Patel and A. Grbic, *IEEE Trans. Microwave Theory and techniques* **62**, 1102, (2014).
[31] R. Courant and D. Hilbert, 1989, *Methods of Mathematical Physics, Volume 2: Differential Equations* (Wiley-Interscience).